13th International Heat Pipe Conference (13th IHPC), Shangai, China, September 21-25, 2004.

# TRANSIENT MODELING OF A CLOSED TWO-PHASE THERMOSYPHON FOR HEAT EXCHANGER APPLICATIONS

**Manfred Molz***
**Marcia B. H. Mantelli**
**Fernando Milanez**
LABSOLAR / NCTS – Departamento de Engenharia Mecânica – Universidade Federal de Santa Catarina
88040-900, Campus Universitário, Florianópolis, SC, Brazil
phone: +55 48 331 9379
* e-mail: mm@labsolar.ufsc.br

**Henrique G. de Landa**
CENPES / PETROBRÁS – Quadra 7, Cidade Universitária
21494-900, Ilha do Fundão, Rio de Janeiro, RJ, BRAZIL

## ABSTRACT

Experimental observations of closed two-phase thermosyphons indicate a transient phenomenon constituted by progression of a heat front coming out of the evaporator and advancing to the condenser's upper end. Depending on operation conditions, this front may stop before reaching the condenser's top, implying a thermally inefficient portion of the thermosyphon, which should be avoided in heat exchanger applications. To describe and explain the transient (and, in the limit, steady state) behavior of this front, also of the active condenser length, a semi-lumped model of the condenser is introduced, which makes uses of Nusselt's condensation analysis as a quasi-static approximation. This model was numerically solved and its main results are presented, the algorithm's coherence having also been tested. An order of magnitude estimate for the transient and steady state behavior of the model's variables was obtained, showing high numerical coherence. Applicability and limitations of the model, based on its assumptions, are also discussed.

**KEY WORDS:** Closed two-phase thermosyphon, transient analysis, heat front, heat exchanger, waste heat recovery

## 1. INTRODUCTION

### 1.1. Heat Exchanger Project and Experiments with CTPT

An estimate was developed concerning the configuration of a heat exchanger employing vertical closed two-phase thermosyphons (CTPT) to air pre-heating through heat recovery from waste gases in an industrial process of Petrobrás. Following this initial design, two carbon steel thermosyphons filled with deionized water were constructed and submitted to experimental investigation. The first of these was filled with a liquid fill rate of $V'$=100% (approx. 908ml) and the other with $V'$=60%.** Their dimensions were: $D_o$=38.2mm, $e$=2.1mm, and a length of 2.2m, divided in: 1m of heating section (evaporator), 1m of cooling section (condenser), and also an intermediate adiabatic section. Heating was provided by cartridge electric resistances inserted in thick annular cooper modules envolving the thermosyphon, the evaporator section being thermally insulated. Cooling by air in natural convection and also by water in forced convection inside a jacket surrounding the condenser were investigated.

Experimental data used to feed our model (presented latter) came out of the first CTPT with a nominal heating power of 1500W and cooling by air, the adiabatic section remaining exposed to ambient air, therefore actuating as a condenser's extension. As these were exploratory experiments, it must not be assumed that the data will be used to an experimental validation of the model.

Some experimental observations pertinent to either thermosyphons follow.

** Please refer to the Nomenclature presented at the end, which gives also some useful definitions.

### 1.2. The Heat Front

Each test begins with the CTPT in thermal equilibrium, then a constant electrical power is applied to the resistances. Heat flux incident upon the evaporator increases gradually because of the interposed cooper thickness. A series of thermocouples distributed over the thermosyphon's entire length allowed the observation of a transient behavior characterized as progression of a heat front that moves along the adiabatic section and then penetrates into the condenser approaching its end cap. The heat front's position can be perceived by very steep temperature increase rates, yet diminishing as the front advances. For relatively low heating powers it stops before reaching the condenser's top. This is specially notable when cooling with water in forced convection, in which case most of the condenser's length can possibly remain at wall temperatures $T_{c,w}$ little above that of water. Meaning that local heat dissipation is comparatively small or even goes to zero on some segment. This can be explained noting that the heat transfer coefficient external to the condenser $h_{c,ext}$ is typically much greater in the case of water in forced convection than with air in natural convection, so that the power incident upon the evaporator is dissipated in a much shorter portion of the condenser.

We emphasize that the hypothesis of this thermosyphon's "cold end" being attributed to greater local heat losses was experimentally eliminated. Also the possibility of it consisting of a region occupied by non-condensable gases can be discarded because for higher heating powers the heat front reaches the end cap.

The hypothesis maintained until now is that the rate of vapor generated in the evaporator $\dot{m}_{e,v}$ is not sufficient to let the vapor reach the condenser higher parts. This implies a limitation on the length in which condensation occurs, that is, on the condensate film length *Lc*. So that maybe it would be more appropriate to speak of a *condensation front*.

Observation of this behavior is important when designing thermosyphon applications because it is related to an inactive portion of the condenser. Which, in the particular case of heat exchangers, is undesirable. That's the motivation for our present modeling work, that until now has been concentrated mainly on the condenser section, seeking to describe the heat front progression and to provide a more rigorous basis with which to confront the hypothesis introduced above.

## 2. MODEL DEVELOPMENT

### 2.1. Proposed Model

In the mathematical model developed we consider the active portion of the condenser (with length *Lc*) as being at a lumped temperature *Tc* in the vapor core and also in the liquid-vapor interface. The liquid film is also assumed to be at a lumped film temperature *Tf*, which is dependent on both *Tc* and an overall temperature of the adjacent wall $T_{c,w}$, set as a boundary condition.

We adopt a formulation of transient processes for open systems (Van Wylen & Sonntag, 1993), with a control volume that is coincident with the condenser's active region, being delimited: laterally by the tube wall; above by the heat front, which is supposed to be flat; and inferiorly by the boundary between adiabatic and condenser sections, also considered as flat.

As a first approximation to model the condensation phenomenon inside the condenser we adopt the analysis developed by Nusselt (*apud* Incropera & DeWitt, 2003; Bejan, 1995). Assumptions on which this analysis is based include among others: **(2.1.a)** the geometry consists of a flat vertical plate; **(2.1.b)** laminar flow in the condensate film; **(2.1.c)** the shear tension between vapor and falling film is negligible; **(2.1.d)** steady state process: no change of variables with time; **(2.1.e)** isothermal wall; **(2.1.f)** advection effects are considered only in the mass conservation equation, implying a linear temperature profile across the film. Letting this last assumption go, on the other hand we include a modification of the vaporization enthalpy as proposed in particular by Rohsenow (*apud* Bejan, 1995, p.408; Incropera & DeWitt, 2003, p.433; Carey, 1992, p.355). Particularly with respect to assumption **(2.1.d)** above, it must be said that our application of Nusselt's analysis is taken as a quasi-static approximation.

In our formulation we include an approximation that either velocities of ascending vapor $v_{e,v}$ and of descending liquid $v_{c,l}$, evaluated at the boundary between adiabatic and condenser sections, are mean velocities. Based on results obtained by Nusselt on his analysis, we make use of three expressions: one for the local film thickness $\delta(y)$; other for the mean film thickness $\overline{\delta}$, given by integration of $\delta(y)$ with respect to *y*, the position

along the film length, and division by the same, *Lc*, being simply $\overline{\delta} = (4/5)*\delta(Lc)$; and another for the local mean velocity $v_{c,l}$, obtained through integration of the local velocity profile $v(x,y)$ with respect to the position $x$ along the local film width $\delta(y)$, divided by $\delta(y)$.

Temporal derivatives of vapor and liquid densities, and of $\overline{\delta}$ were left out the conservation equations. Effects of thermal resistance and heat accumulation on tube wall were also disconsidered. So our problem is formulated by the system of mass and energy conservation equations specified as follows:

$$m_c' \frac{dLc}{dt} = \dot{m}_{e,v} - \dot{m}_{c,l} \quad \text{(CM)}$$

$$m_c' \left( u_c \frac{dLc}{dt} + Lc \frac{du_c}{dt} \right) = h_{e,v}\dot{m}_{e,v} - h_{c,f}\dot{m}_{c,l} - q_{c,w} \quad \text{(CE)}$$

Equations CM and CE are both constituted of vapor and liquid advection terms, with mass flow rates given respectively by

$$\dot{m}_{e,v} = \rho_{e,v}.v_{e,v}.A_{c,v} \quad (1)$$

$$\dot{m}_{c,l} = \rho_{c,f}.v_{c,l}.A_{c,l} \quad (2)$$

where the cross-sectional areas of flow are

$$A_{c,v} = \pi.(R_i - \delta)^2 \quad (3)$$

$$A_{c,l} = \pi.R_i^2 - \pi.(R_i - \delta)^2 \quad (4)$$

and of the accumulation terms – represented by the left side of each equation, where

$$m' = \rho_{c,f}\overline{A}_{c,l} + \rho_{c,v}\overline{A}_{c,v} \quad (5)$$

– whose mean cross-sectional areas of liquid $\overline{A}_{c,l}$ and vapor $\overline{A}_{c,v}$ are the same as (3) and (4) but with $\overline{\delta}$ in the place of $\delta$. Furthermore, the CE equation has a term accounting for the diffusive heat transfer, accounting for the rate of heat dissipated from the condenser, $q_{c,w} = q''_{c,w}.A_{c,w}$, where

$$q''_{c,w} = h_{c,ext}.(T_{c,w} - T_\infty) \quad (6)$$

$$A_{c,w} = 2.\pi.R_o.Lc \quad (7)$$

The internal energy of the control volume is evaluated through $u_c = (1\text{-}x_c).u_{c,f} + x_c.u_{c,v}$, where $x_c$ is the thermodynamic title, given by $\rho_{c,v}.\overline{A}_{c,v}/(\rho_{c,f}.\overline{A}_{c,l} + \rho_{c,v}.\overline{A}_{c,v})$.

### 2.2. Thermophysical Properties Evaluation, Boundary and Initial Conditions

Thermophysical properties of vapor ascending from the evaporator and of vapor in the control volume, both supposed to be saturated, are evaluated respectively at the evaporator temperature *Te* and at *Tc*. The vaporization entalphy is evaluated at *Tc*, too. Liquid properties, both in the control volume and crossing the boundary downwards, are evaluated at the film temperature $T_f = (Tc+T_{c,w})/2$ (Bejan, p.408, p.415). Which is the meaning of the subscript *f* appearing along with liquid properties. Despite the fact that the liquid in the falling film is subcooled except at the liquid-vapor interface, an approximation is made to consider it saturated at $T_f$.

Formulation of functions to approximate the relevant thermophysical properties of liquid and vapor in terms of the saturation temperature was based on lists of values generated in the *EES* software. In the case of $u_{c,f}$ and $u_{c,v}$, no approximation functions were created, since the respective lists were stored each in a file and read at every evaluation. Furthermore, it was assumed the same geometry of the experimented CTPT ($D_o$ and $e$), $g$=9.807m/s$^2$, and $T_\infty$=25$^o$C.

A number of functions corresponding to the boundary conditions assumed as known were formulated on base of experimental data (see Figures 1 and 2) obtained from the situation of cooling through air in natural convection (as already mentioned). This choice is owned to the fact that in such situation: **(a)** temperature distribution $T_{c,w}(y)$ is closer to an isothermal wall condition than with water in forced convection; and **(b)** the transient is slower, what comes closer to our quasi-static approximation. According to this situation, it was postulated that $h_{c,ext}$=20W/m$^2$.$^o$C.

The functions of time approximated from the data were $T_{c,w}$, *Te* (Figure 2) and, provisionally, the active condenser length *Lc(t)* itself (Figure 1). Which value is coincident to the heat front position measured from the boundary between condenser and adiabatic sections.

As initial conditions (in $t$=0s) we assume: $Tc=T_\infty$ (thermal equilibrium); $x_c$=1; and $Lc$=0.

### 2.3. Solution Approaches

The system of equations CM + CE was numerically solved by way of two different approaches:

**I**. With knowledge of the heat front position *Lc(t)*, *Tc* and $v_{e,v}$ were calculated.

**II**. Once $\dot{m}_{e,v}$ is considered to be known (equivalent, for pratical purposes, to knowig $v_{e,v}$), *Tc* and *Lc* can then be calculated.

To take *Lc* as an input variable in approach **I** makes it possible to obtain results of $v_{e,v}$ that at least permits one to have an order of magnitude estimate for that variable. (Also, within the limitations of model and boundary conditions assumed.) But our objective is to determine the heat front position *Lc*

(*i.e.*, the condenser active length) over time, and particularly in steady state, without first prescribing *Lc*. Because this implies to indirectly prescribe $v_{e,v}$ too.
So, to use approach **II** directly would demand: or **(a)** that values of $v_{e,v}$ should be entered after obtained experimentally; which is difficult and little viable in practice, because of measurement difficulties, and also because it is not an usual (controllable) experimental parameter, as would more properly be the case of $q_{e,w}$, the heat rate input in the evaporator; or **(b)** that such information should be obtained by modeling the condenser coupled to the evaporator and including thermal exchanges between them and the environment, which could be more easily acquired as experimental data.

### 2.4. Search for Solutions and Convergence

A totally implicit scheme of solution was adopted, that is: all variables are evaluated at present time *t*, and those involved in the derivatives also assuming the values calculated at the previous time, $t - \Delta t$ (Maliska, 1995). Either the variable derivatives with respect to time were approximated by finite differences, when the function that represents the variable was not known (which is the case of $u_c$ in approach **I** and also of *Lc* in approach **II**); or directly obtained by calculating the derivative of the function (the case of *Lc* in approach **I**).

To obtain the solutions for the two unknowns in either approaches, an exhaustive search method (Stoecker, 1989) was implemented in *Maple*. Since the condenser core temperature *Tc* must necessarily lie between *Te* and $T_{c,w}$, this temperature interval was divided in a certain number of segments (10, in our case) and, beginning from $Tc=T_{c,w}$, the values of the other unknown (either $v_{e,v}$ or *Lc*) as calculated by each of the two equations, CM and CE, were compared. Two temperatures adjacent in the interval are searched so that: at one, say, *Tc[i]*, the unknown calculated by CM is greater (or smaller) than the one calculated by CE; and, at the other one, *Tc[i+1]*, this relation is inverse. Once this is achieved, the corresponding segment is subdivided again, and so on. The iterations for a given time step cease after a number *K* of repetitions of this procedure. This number is estipulated so that the difference between mean values calculated in *i* and *i+1*, and also the difference between the values calculated through each equation for both *i* and *i+1*, are considered small enough. (The relative differences were typically of $\sim 10^{-10}$ or smaller.)

## 3. RESULTS AND DISCUSSION

For the results that follow, a time step $\Delta t$=30s was adopted. Until *t*=900s a value of *K*=20 was postulated, and after that *K*=12. In *Maple* it was defined that the floating point numbers would be handled with 25 digits.
In Figure 1 below are presented: the points taken out of the experimental data to represent the heat front position over time; the continuous function *Lc(t)* created to approximate these points; e some points of the unknown *Lc* simulated through sucessive application of approaches **I** and **II**.

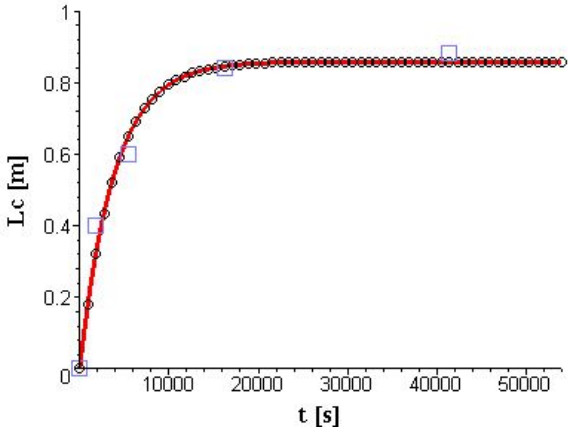


Figure 1. Heat front locations over time (large squares), *Lc(t)* function approximated from this points (continuous line), and sample points of numerical results obtained for *Lc* (small circles).

The objetive of this last procedure is to verify the simulation algorithm's coherence. First the $v_{e,v}$ results calculated by approach **I** are stored in a file as function of *Tc*. Then approach **II** iteractively takes as input $v_{e,v}$ values interpolated according to each try of *Tc*.
Differences between the postulated function *Lc(t)* and the *Lc* values calculated by approach **II** showed a dispersion in the range of $\pm 10^{-10}$m.

Following are numerical results obtained by application of approach **I**, presented in graphical form. To all effects, the same graphics could also be presented after sucessive application of approach **II**, as exemplified by the very narrow range of dispersion of differences between results from each approach, just mentioned above.
To simplify the exposition of results some dimensionless variables are created, whose

definitions are given along the text. Note that the variables mentioned in the figures, particularly as labels of the curves, are more like references and don't correspond necessarily to the variables plotted.

First we define a dimensionless temperature $\theta=(Tc - T_{c,w})/(Te - T_{c,w})$. In figure 2 a curve of θ multiplied by 25 is shown, and also other temperature curves which are all adimensionalized dividing them by 250°C. It can be noted that $Tc$ is much closer to $T_{c,w}$ than to $Te$. More exactly, the value of θ*100 amounts to ~2.5%, or also $(Tc - T_{c,w}) \approx 0.28$°C, as $t \to \infty$.

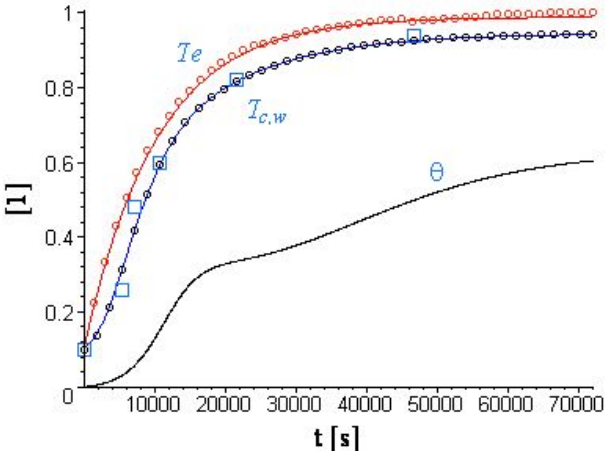


Figure 2. Adimensionalized plots of: prescribed functions $Te$ and $T_{c,w}$ (continuous lines labelled); some experimental points for approximation of these functions (respectively small circles near $Te$ and large squares near $T_{c,w}$); some $Tc$ numerical points (circles over $T_{c,w}$); and a curve of θ*25.

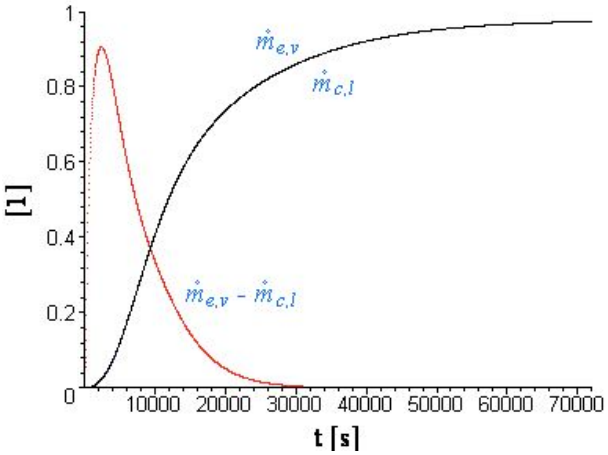


Figure 3. Adimensionalized plots of $\dot{m}_{e,v}$, $\dot{m}_{c,l}$, and $(\dot{m}_{e,v} - \dot{m}_{c,l})$ *versus* $t$.

The adimensional curves in Figure 3 were obtained dividing $\dot{m}_{e,v}$ and $\dot{m}_{c,l}$ by $2.5*10^{-4}$kg/s, and $(\dot{m}_{e,v} - \dot{m}_{c,l})$ by $2.5*10^{-7}$kg/s. The difference between $\dot{m}_{e,v}$ and $\dot{m}_{c,l}$ is so small that it practically makes no difference to plot both curves together. In fact, they differ in $\sim 10^{-7}$kg/s. Also, practically the same curve of the difference $(\dot{m}_{e,v} - \dot{m}_{c,l})$ as seen in Figure 3 was also obtained by plotting the calculated points corresponding to the accumulation term on the left side of CM.

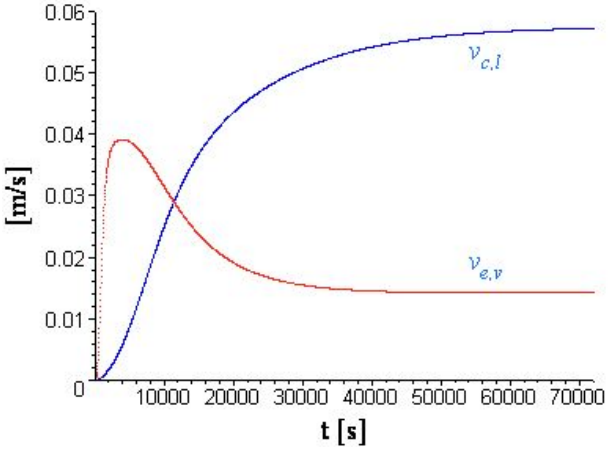


Figure 4. Velocities of vapor $v_{e,v}$ and liquid $v_{c,l}$.

In Figure 4 one can see that $v_{e,v}$ reaches a maximum and after that diminishes asymptotically. Roughly this is due to the rate of increase of $\rho_{e,v}$ with $Te$, which is greater than that of $\dot{m}_{e,v}$ (*vide* Figure 3), implying a decrease in $v_{e,v}$. (The variation of $A_{c,v}$ can be neglected since $\overline{\delta}$ has a magnitude order of $\sim 4*10^{-5}$m for $t > 0$.)

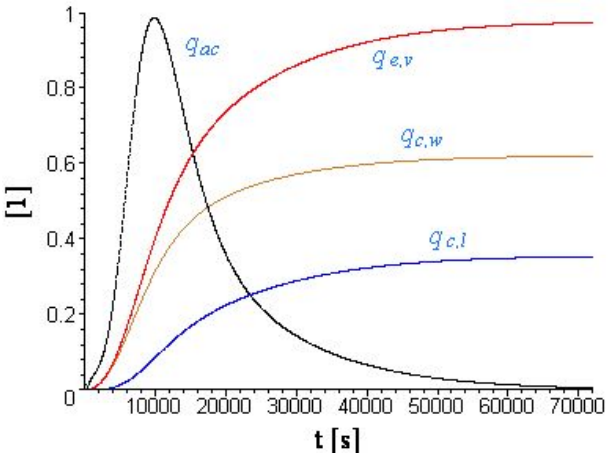


Figure 5. Adimensionalized heat rates of: advection of vapor $q_{e,v}$ and of liquid $q_{c,l}$; dissipation from the condenser $q_{c,w}$; and accumulation $q_{ac}$.

The curve of energy accumulation rate $q_{ac}$ in Figure 5 was obtained by subtracting $q_{c,w}$ and $q_{c,l} = \dot{m}_{c,l}.h_{c,f}$ from $q_{e,v} = \dot{m}_{e,v}.h_{e,v}$ and dividing this by 0.7W. The others curves were obtained dividing the respective heat rates by 700W. Practically the same $q_{ac}$ curve

was obtained calculating directly the left side of CE (accumulation term) based also on the numerical results. The value of $q_{ac}$ is comparatively very small near the other terms in CE; in fact, less than 1% of any of these for $t$ >0 (in a scale-analysis sense). So we have $\dot{m}_{e,v}.h_{e,v} - \dot{m}_{c,l}.h_{c,f} \approx q_{c,w}$. This difference is more exact as $t\to\infty$ because then $q_{ac}\to 0$ (see Figure 5).

Since we are applying results from approach **I**, $q_{c,w}$ is prescribed as a function of time because *Lc(t)* and $T_{c,w}$ are so, and also $h_{c,ext}$ is fixed. When $t\to\infty$, $q_{c,w}$ will be equal to the rate of heat transported by the CTPT in permanent regime.

A sensibility analysis to $h_{c,ext}$ was performed, in which that variable assumed the values 10, 20, and 40W/m$^2$.$^o$C. Some selected results for $t$=72000s (nearly $t\to\infty$), that is, as the condenser approaches steady state operation, are summarized in Table 1 below. The transient curves of $v_{e,v}$ for each $h_{c,ext}$ value are presented in Figure 6.

Table 1. Influence of $h_{c,ext}$ on selected variables for $t$=72000s.

| $h_{c,ext}$ [W/m$^2$.$^o$C] | $q_{c,w}$ [W] | $Tc$-$T_{c,w}$ [$^o$C] | $v_{e,v}$ [m/s] | $\bar{\delta}$ *10$^{-5}$ [m] |
|---|---|---|---|---|
| 10 | 218 | 0.11 | 0.007 | 3.1 |
| 20 | 435 | 0.28 | 0.014 | 3.9 |
| 40 | 870 | 0.70 | 0.029 | 4.9 |

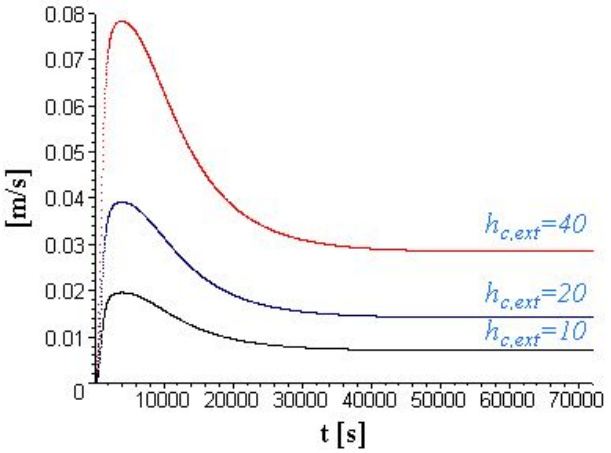


Figure 6. Vapor velocity $v_{e,v}$ for various $h_{c,ext}$.

In Figure 6 it can be noted that $v_{e,v}$ is nearly proportional to $h_{c,ext}$ for $t$ >0. In fact we have $q_{c,w} \propto h_{c,ext}$. An increase in $h_{c,ext}$, and so in $q_{c,w}$, implies that there must be a greater condensation rate and also an increase in $\dot{m}_{e,v}$. Which means almost a direct effect on $v_{e,v}$, since the other factores are unimportant ($A_{c,v}$≈constant and $\rho_{e,v}$ depends on $Te$).

Based on numerical results from the present model, the neglected mass accumulation term including the temporal derivatives of both densities of vapor and of liquid was considered. As a first estimate, it was found that this supressed accumulation term of the CM equation is ~$10^{-7}$kg/s, *i.e.*, the same magnitude order as the accumulation term included in CM. This magnitude order is that of the term involving the vapor density derivative. The term of the liquid density derivative being at most ~$10^{-8}$kg/s.

Heat diffusion across the heat front was neglected in the model. To consider it is more important when in steady state or near it, when the heat front becomes stationary and the greater temperature differences occur between active and inactive regions of the condenser. In fact, it was observed that the frontier between them is progressively characterized by a transition region with temperatures intermediate to $Tc$ and $T_\infty$.

Nusselt's analysis as applied to our model will now be discussed, following the assumptions as enumerated in subsection **2.1.**: **(2.1.a)** Its validity can be extended to other geometries since the supposition of "thin" film be applicable. In our present case of condensation inside a round tube, this implies that $\bar{\delta} << D_i$ (*vide* Bejan, pp.412-413), which is satisfied since we have $\bar{\delta}/D_i \sim 10^{-4} << 1$. **(2.1.b)** Film condensation with laminar flow can be sustained up to $Re_{Lc}$~30 (Bejan, p.411). As $t\to\infty$ in our simulation, we calculated $Re_{Lc}\approx$ 84, so we should expect that part of the film would present a wavy flow pattern (until $Re_{Lc}\sim$ 1800, suggests Bejan). **(2.1.c)** The magnitude of shear stress at the liquid-vapor interface was not verified, and also not up to which point it can be neglected. **(2.1.d)** It is uncertain until which point and how great the error implied in considering that the transient condensation process can be modeled assuming it as occurring in steady state. **(2.1.e)** The application of the model to situations in which the distribution $T_{c,w}(y)$ is little uniform is doubtful, but probably would require a longitudinal discretization of the condenser.

## 4. CONCLUSIONS AND CONTINUATION

Results presented so far should be viewed as of qualitative nature.

The inclusion of the density derivatives in the accumulation terms of both CM and CE is to be done in sequence.
The proposed model is also to be submitted to more accurate experimental data, with which new boundary conditions should be formulated, including $h_{c,ext}$.
However, with the present experimental apparatus it's possible to compare model results near steady state with *Tc* data obtained from readings of an internal thermocouple projected inside the superior region of the condenser through its end cap. To that end, the wall thermal resistance should be included, since it implies a temperature difference which is of same magnitude order than that across the film. The power transported in steady state as calculated by the model and as obtained experimentally can also be compared.

In continuation of this work, the present condenser model should be extended as to include the evaporator, in a way that $v_{e,v}$ (or $\dot{m}_{e,v}$) will be a coupling condition between the evaporator and condenser sections (if the adiabatic section is disconsidered).

## NOMENCLATURE

$A$ area [$m^2$]
$\overline{A}$ mean area (based on $\overline{\delta}$) [$m^2$]
$D$ tube diameter [m]
$e$ tube wall thickness [m]
$g$ gravitational acceleration [$m/s^2$]
$h$ specific enthalpy [J/kg]
$h_{c,ext}$ condenser external heat transfer coefficient [$W/m^2.^oC$]
$i$ iteration step [1]
$K$ number of subdivisions of searched interval [1]
$Lc$ active condenser length; heat front position (origin at condenser-adiabatic sections boundary) [m]
$\dot{m}$ mass flowrate [kg/s]
$m'$ mass per unit length [kg/m]
$q$ heat rate [W]
$q''$ heat flux [$W/m^2$]
$Re_{Lc}$ local Reynolds number of liquid film ($=4.\rho_{c,f}.v_{c,l}.A_{c,l}/\mu_f$) [1]
$R$ tube radius [m]
$t$ time [s]
$T$ temperature [$^oC$]
$Tc$ condenser lumped temperature [$^oC$]
$Te$ evaporator lumped temperature [$^oC$]
$T_{c,w}$ condenser wall temperature [$^oC$]
$u$ specific internal energy [J/kg]
$v$ velocity (in the vertical direction) [m/s]
$V'$ liquid fill rate: ratio of liquid volume (at 20$^o$C and 1atm) to evaporator volume [1]
$x$ film thickness coordinate (origin at inner wall surface) [m]
$x_c$ thermodynamic quality [1]
$y$ film vertical coordinate (origin at $\delta(y)$=0) [m]
$\delta$ film thickness [m]
$\overline{\delta}$ mean film thickness [m]
$\Delta t$ time step [s]
$\rho$ density [$kg/m^3$]
$\theta$ adimensional temperature difference [1] ($=(Tc - T_{c,w})/(Te - T_{c,w})$)

### Subscripts

| | | | |
|---|---|---|---|
| *ac* | accumulated | *l* | saturated liquid |
| *c* | condenser | *o* | outer |
| *e* | evaporator | *v* | saturated vapor |
| *ext* | external | *w* | wall |
| *f* | film | $\infty$ | property of reservoir fluid |
| *i* | inner | | |

### Relational symbols

| | | | |
|---|---|---|---|
| $\sim$ | order of magnitude | * | multiplication |
| $\approx$ | approximately | $\propto$ | proportionality |

## REFERENCES


1. Van Wylen, G. J., Sonntag, R. E., *Fundamentos da Termodinâmica Clássica*, Edgard Blücher Ltda., São Paulo, 1993, 3ª ed.
2. Bejan, A., *Convection Heat Transfer*, John Wiley & Sons, Inc., 1995, 2nd ed.
3. Stoecker, W. F., *Design of Thermal Systems*, Mc-Graw-Hill, Inc., 1989, 3rd ed.
4. Maliska, C. R., *Transferência de Calor e Mecânica dos Fluidos Computacional*, LTC S.A., Rio de Janeiro, 1995.
5. Incropera, F. P., DeWitt, D. P., *Fundamentos de Transferência de Calor e Massa*, LTC S.A., Rio de Janeiro, 2003, 5ª ed.
6. Carey, van P., *Liquid-Vapor Phase-Change Phenomena – an Introduction to the Thermophysics of Vaporization and Condensation Processes in Heat Transfer Equipment*, Taylor & Francis, 1992.